Computers and Geotechnics 36 (2009) 503–516

Contents lists available at ScienceDirect

Computers and Geotechnics

journal homepage: www.elsevier.com/locate/compgeo

ANN-based model for predicting the bearing capacity of strip footing on multi-layered cohesive soil

Y.L. Kuo [a], M.B. Jaksa [a,*], A.V. Lyamin [b], W.S. Kaggwa [a]

[a] School of Civil, Environmental and Mining Engineering, The University of Adelaide, SA 5005, Australia
[b] Department of Civil Surveying and Environmental Engineering, The University of Newcastle, University Drive, Callaghan, NSW 2308, Australia

ARTICLE INFO

Article history:
Received 25 January 2007
Received in revised form 14 April 2008
Accepted 28 July 2008
Available online 10 September 2008

Keywords:
Bearing capacity
Cohesive soil
Limit analysis
Multilayered cohesive material
Strip footing
Neural network

ABSTRACT

In reality, footings are most likely to be founded on multi-layered soils. The existing methods for predicting the bearing capacity of 4-layer up to 10-layer cohesive soil are inaccurate. This paper aims to develop a more accurate bearing capacity prediction method based on multiple regression methods and multi-layer perceptrons (MLPs), one type of artificial neural networks (ANNs). Predictions of bearing capacity from the developed multiple regression models and MLP in tractable equations form are obtained and compared with the value predicted using traditional methods. The results indicate ANNs are able to predict accurately the bearing capacity of strip footing and outperform the existing methods.

1. Introduction

The ultimate bearing capacity of a shallow strip footing founded on a single homogenous soil layer is usually calculated using Terzaghi's equation [1]:

$$q_u = cN_c + qN_q + \frac{1}{2}\gamma N_\gamma B \quad (1)$$

where N_c, N_q and N_γ are the dimensionless bearing capacity factors. c is undrained shear strength of the soil (kPa), q is the surcharge (kN/m^2), γ is the unit weight of soil (kN/m^3) and B is the footing width (m).

For a strip footing founded on a single homogenous layer of cohesive soil, assuming the soil is weightless and without surcharge, the ultimate bearing capacity becomes:

$$q_u = N_c c \quad (2)$$

N_c is given by Prandtl solution, which is equal to $2 + \pi$ or 5.14 [2].

In reality, most naturally occurring soils are formed in discrete layers and are often heterogenous. Therefore, footings are most likely to be founded on heterogenous and multi-layered soils, in which the soils' strength may increase or decrease with depth, or the soil profile may consist of distinct layers having significantly different properties. The effect of increasing strength on bearing capacity has been addressed by Davis and Booker [3], while rigorous solutions to the problem of strip footings founded on two-layered cohesive soils were obtained by several researchers, notably Button [4]; Chen [5]; Reddy and Srinivasan [6]; Brown and Meyerhof [7]; Meyerhof and Hanna [8]; Burd and Frydman [9]; Florkiewicz [10] and more recently, Merifield et al. [11]. However, determination of the bearing capacity of footing on multi-layered, cohesive soils remains empirical. For example, Bowles [12] suggested using the weighted average soil strength, c_{av}, of a number of cohesive layers as follows:

$$c_{av} = \frac{\sum_{i=1}^{n} c_i h_i}{\sum_{i=1}^{n} h_i} \quad (3)$$

where n is the total number of layers; c_i and h_i, respectively, represent the soil cohesion and the thickness of the ith stratum. The $\sum_{i=1}^{n} h_i$ is calculated as follow:

$$\sum_{i=1}^{n} h_i = 0.5 \times B \times \tan(45 + \phi) \quad (4)$$

where ϕ is the internal frictional angle of soil, which, in this case, is equal 0°.

The bearing capacity problem, which is considered in this paper, is illustrated in Fig. 1. A strip footing, of width B, is founded on a number of thin, horizontal layers having thickness, h_i, and soil cohesion, c_i. The ultimate bearing capacity, q_u, can then be expressed as

* Corresponding author. Tel.: +61 8 8303 4317; fax: +61 8 8303 4359.
E-mail address: mjaksa@civeng.adelaide.edu.au (M.B. Jaksa).

0266-352X/$ - see front matter © 2008 Elsevier Ltd. All rights reserved.
doi:10.1016/j.compgeo.2008.07.002

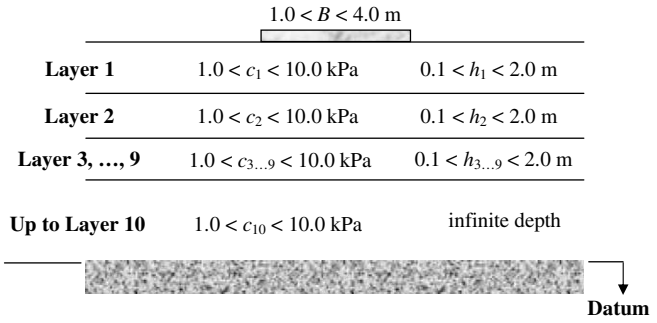

Fig. 1. Problem definition for 10-layered cohesive soil.

$$q_u = f(c_i, h_i, B) \tag{5}$$

A rigorous method that can be used for predicting the collapse load is the displacement finite element method (DFEM). Theoretically, this technique can deal with complex loadings, excavation and deposition sequences, geometries of arbitrary shape, anisotropy, layered deposits and complex stress–strain relationships. However, experience has indicated that the results from DFEM tend to overestimate the true limit load and, in some instances, fail to provide a clear indication of the collapse load altogether [13,14]. This phenomenon, which is commonly known as 'locking', arises when the displacement field becomes over-constrained by the requirement of an incompressible plastic flow rule. As a result, this restricts the type of element that may be used successfully in limit load computations.

2. Numerical formulation of limit analysis

The methods that are used in this paper for determining the bearing capacity of multi-layered soil, are the numerical formulation of upper and lower bound methods. These numerical techniques were developed by Lyamin and Sloan [15,16], based on the limit theorems of classical plasticity and finite elements. The methods assume a rigid-plastic soil model with a Mohr–Coulomb yield criterion and subsequently, this assumption leads to non-linear programming problem. The solution to the kinematic optimisation problem defines a kinematically admissible velocity field and, thus, yields a rigorous upper bound to the bearing capacity of a foundation. The solution to the static optimisation problem defines a statistically admissible stress field and results in a rigorous bearing capacity lower bound. The limit theorems, when employed, can bracket the true collapse load from above and below [15,16].

In this study, the numerical formulation of the upper and lower methods are used conduct a series of parametric studies to examine the factors (c_i, h_i and B) influencing the ultimate bearing capacity (q_u), and to develop a meta-model to more accurately predict the bearing capacity of multi-layered cohesive soils. The meta-model is based on a type of artificial neural network (ANN) known as a back-propagation, multi-layer perception (MLP). The results of parametric studies from the numerical limit simulations are used to train the MLP models. The performance of several MLP models is measured by three different performance measures, and compared to other methods. Parametric studies on MLP models are also carried out to assess the robustness of the proposed models. An illustrative numerical example is also presented in the paper.

The numerical implementation of the lower and upper bound analyses for two-dimensional problems discretizes the soil mass into three-noded triangular elements. In contrast to conventional displacement finite element analysis, each node is unique to a particular element, although several nodes share the same coordinates. For the lower bound formulation, each node is associated with three unknown stresses, and these are assumed to vary linearly. A stress discontinuity can occur along the shared edge between elements, and at all points along the discontinuity, the shear and normal tractions must be in equilibrium.

After assembling the various objective function coefficients and equality constraints for the mesh and imposing the non-linear yield inequalities on each of the nodes, the lower bound formulation of Lyamin and Sloan [16] leads to a non-linear programming problem of the form:

$$\begin{aligned} &\text{maximise} && \mathbf{c}^{\mathrm{T}}\boldsymbol{\sigma} \\ &\text{subject to} && \mathbf{A}\boldsymbol{\sigma} = \mathbf{b} \\ & && f_i(\boldsymbol{\sigma}) \leqslant 0, \quad i = \{1, \ldots, N\} \end{aligned} \tag{6}$$

where c is a vector of the objective function coefficients, $\boldsymbol{\sigma}$ is a vector of the unknowns (nodal stresses and unit weights), $\mathbf{c}^{\mathrm{T}}\boldsymbol{\sigma}$ is the collapse load, $\mathbf{A}$ is a matrix of the equality constraint coefficients, $\mathbf{b}$ is a vector of coefficients, f_i is the yield function for node i and N is the number of nodes [16].

For the upper bound formulation, however, each node is associated with two unknown velocities and each element has p non-negative multiplier rates, where p is the number of sides in the linearized yield criterion. A linear variation of velocities is assumed within each triangular element. For each velocity discontinuity, there are also four non-negative discontinuity parameters that describe the velocity jumps along each edge of the triangle.

Once the constraints and the objective function coefficients are assembled, the task of finding a kinematically admissible velocity field, which minimises the internal power dissipation for a specified set of boundary conditions, may be written as

$$\begin{aligned} &\text{maximise} && \boldsymbol{\sigma}^{\mathrm{T}}\mathbf{B}\mathbf{u} + \mathbf{c}_{\mathbf{u}}^{\mathrm{T}}\mathbf{u} + \mathbf{c}_{\mathbf{d}}^{\mathrm{T}}\mathbf{d} \quad \text{on } (\boldsymbol{\sigma}) \\ &\text{minimise} && \boldsymbol{\sigma}^{\mathrm{T}}\mathbf{B}\mathbf{u} + \mathbf{c}_{\mathbf{u}}^{\mathrm{T}}\mathbf{u} + \mathbf{c}_{\mathbf{d}}^{\mathrm{T}}\mathbf{d} \quad \text{on } (\mathbf{u}, \mathbf{d}) \\ &\text{subject to} && \mathbf{A}_{\mathbf{u}}\mathbf{u} + \mathbf{A}_{\mathbf{d}}\mathbf{d} = \mathbf{b} \\ & && f_i(\boldsymbol{\sigma}) \leqslant 0, \quad i = \{1, \ldots, E\} \\ & && \mathbf{d} \geqslant 0 \end{aligned} \tag{7}$$

where $\mathbf{u}$ is a global vector of unknown velocities; $\mathbf{d}$ is a global vector of unknown discontinuity variables; $\boldsymbol{\sigma}$ is a global vector of unknown element stresses; $\mathbf{c}_{\mathbf{u}}$ and $\mathbf{c}_{\mathbf{d}}$ are vectors of objective function coefficients for the nodal velocity and discontinuity variables, respectively; $\mathbf{A}_{\mathbf{u}}$ and $\mathbf{A}_{\mathbf{d}}$ are matrices of equality constraints coefficients for the nodal velocities and discontinuity variables, respectively; $\mathbf{B}$ is a global matrix of compatibility coefficients that operate on the nodal velocities; and $\mathbf{b}$ is a vector of coefficients. In this equation, the objective function, $\boldsymbol{\sigma}^{\mathrm{T}}\mathbf{B}\mathbf{u} + \mathbf{c}_{\mathbf{u}}^{\mathrm{T}}\mathbf{u} + \mathbf{c}_{\mathbf{d}}^{\mathrm{T}}\mathbf{d}$, denotes the total dissipated power, with the first term giving the dissipation in the continuum, the second term giving the dissipation due to fixed boundary tractions or body forces, and the third term giving the dissipation along the discontinuities [15].

The solutions to Eqs. (6) and (7) can be found efficiently by solving the system of non-linear equations that define its Kuhn–Tucker optimality. It is reported that the proposed two-stage quasi-Newton solver [17] requires less than approximately 50 iterations, regardless of the problem size, and the resulting algorithm is many times faster than an equivalent one based on linear programming [15,16]. The solutions of the lower and upper bound computations bracket the actual collapse load from below and above, and thus give a clear indication of the accuracy of the results.

3. Overview of back-propagation multi-layer perceptrons

A comprehensive description of back-propagation multi-layer perceptrons (MLPs) is beyond the scope of this paper and can be found in many publications (e.g. [18,19]). In addition, the application of ANNs in the field of geotechnical engineering is discussed in

some detail by Shahin et al. [20]. The typical structure of a MLP model consists of a number of processing elements (PE) or nodes, that are usually arranged in layers: an input layer, an output layer and one or more hidden layers. Each PE in a specific layer is fully or partially joined to many other PEs via weighted connections. The input from each PE in the previous layer (x_i) is multiplied by an adjustable connection weight (w_{ji}). At each PE, the weighted input signal is summed and a threshold value or bias (θ_j) is added or subtracted. This combined input (I_i) is then passed through a non-linear transfer functions ($f(\cdot)$) (e.g. a sigmoidal or tanh functions) to produced the output of the PE (y_i). The output of one PE provides the input to the PEs in the next layer. This process is summarised in Eqs. (8) and (9) and illustrated in Fig. 2:

$$\text{Summation} \quad I_j = \sum (w_{ji} x_i) + \theta_j \tag{8}$$

$$\text{Transfer} \quad y_j = f(I_j) \tag{9}$$

The propagation of information in the MLP starts at the input layer, where the network is presented with an actual measured set of input data. The actual output of the network is compared with the desired output and an error is calculated. Using this error and utilising a learning rule, the network adjusts its weights until some stopping criterion is met, so that the network can obtain a set of weights that will produce the input/output mapping that provides the smallest possible error. This process is known as "learning" and "training". One common stopping criterion, that will be used for development of MLP model in this paper, is the cross-validation technique proposed by Stone [22], which is considered to be most valuable tool to ensure that overfitting does not occur [23]. Cross-validation requires the data be divided into three sets: training, testing and validation. The training set is used to adjust the connection weights, and the testing set is used to determine when to stop training to avoid overfitting. The validation is set is used to test the predictive ability of the model in the deployed environment.

4. Data generation using numerical formulation of upper and lower bound theorem

To generate data for developing bearing capacity equations for multi-layered soil, a parametric study is required to carried out that examines each of the factors influencing the bearing capacity. This is needed for both multi-regression analysis, and also to train and test the MLP models. The bearing capacity problems considered in this study were illustrated previously in Fig. 1. A rough shallow strip footing founded on multi-layered cohesive, soils with cohesion, c_i, ranging from 1.0 to 10.0 kPa. The width of the footing, B, is assumed to vary between 1.0 and 4.0 m, and the thickness of each of the layers, h_i, varies in between 0.1 and 2.0 m, except for the last layer in each case, i.e. h_4 in 4-layer case and h_{10} in 10-layer case, which is assumed to have infinite depth.

To achieve a tight bracket between the lower and upper bounds, very fine meshes have been used, and typical upper and lower bound meshes for a strip footing resting on a multi-layered soil are shown in Figs. 3 and 4, respectively. Both the upper and lower bound computations are carried out on half of the domain due to the symmetric nature of the problem. The size of the meshes used in the upper and lower bound computations are set to $5 \times B_{max}/2$ (i.e. 10.0) m in depth and $5 \times B_{max}/2$ (i.e. 10.0) m in width, to ensure that the meshed domain contains the plastic zone. In lower bound computation, special "extension" elements are also placed on part of the boundary of the stress field (Fig. 3) to model the unbounded domain, thus providing a complete statically-admissible stress field and a rigorous lower bound.

The footing is modelled as a rough footing and, as a result, a special line element is included in the upper bound computations to create a series of velocity discontinuities between the footing base and soil, which can be assigned a suitable strength value, enabling various type of footing problem to be analyzed. For example, for a perfectly rough footing case, the velocity discontinuities are assigned a strength equal to the undrained shear strength of the soil. To model a perfectly rough footing in the lower bound computation, no additional constraints are placed on the allowable shear stress at element nodes located directly beneath the footing. The shear stress is, therefore, unrestricted and may vary up to the undrained shear strength of the soil (according to the yield constraint) [16].

A series of 2000 realizations of Monte Carlo simulation are carried out on each of the factors that affect bearing capacity. For each realization, values of c_i, B, h_i are randomly selected from a uniform distribution within pre-defined ranges, and presented as inputs for the numerical limit simulations. The upper and lower bound solutions, denoted by q_u^{UB} and q_u^{LB}, respectively, are obtained and shown in Figs. 5 and 6. The error, which measures the accuracy of the solutions, is defined as

$$\text{Error} = \frac{q_u^{UB} - q_u^{LB}}{q_u^{UB} + q_u^{LB}} \times 100 \tag{10}$$

The error ranged between ±0.5% and ±24.6% with an average of ±2.6%, indicating that the bounds were very tight. However, large errors arise when a very thin (e.g. 0.1 m) and soft (e.g. 1.0 kPa) uppermost clay layer is underlain by a very stiff (e.g. 10 kPa) layer. Such errors, however, do not affect the overall accuracy of the proposed model, as only 0.06% of the population (i.e. 12 out of 2000) had an error, which exceed ±10.0%, and 95.9% of the population

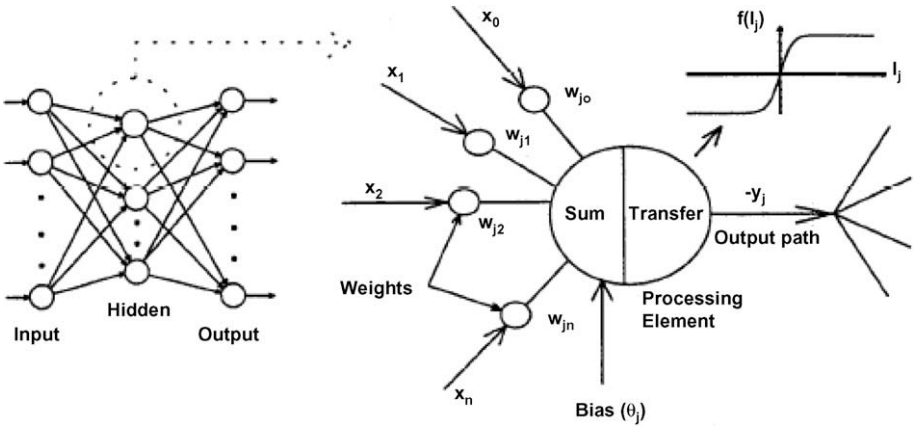

Fig. 2. Typical structure and operation of ANNs [21].

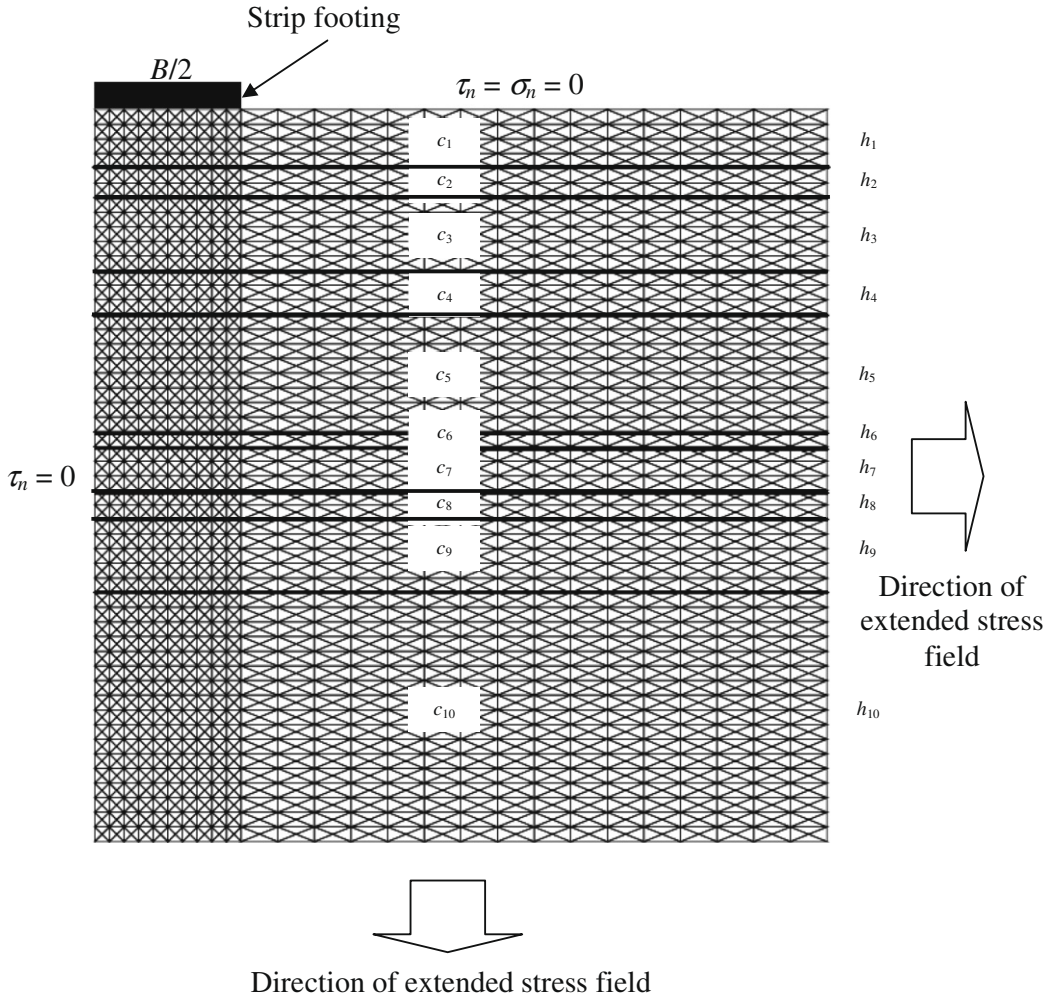

Fig. 3. Typical mesh for analysis of strip footing and directions of extensions for lower bound implementation.

had an error below ±5.0%. Hence, it is reasonable to adopt the average values of the upper and lower bound solutions as the exact collapse loads, as the range is small in most cases.

5. Multiple-regression analysis

Multiple-regression is used to develop a relationship between the single dependent variable, q_u, and one or more independent variables c_i, h_i and B. For 4-layered soils, the prediction of q_u is accomplished by the following equation:

$$q_u = w_1c_1 + w_2c_2 + w_3c_3 + w_4c_4 + w_5h_1 + w_6h_2 + w_7h_3 + w_8B + b \quad (11)$$

where w_i are the regression weights and are computed in a manner that minimises the sum of the squared deviations; and b is the y-axis intercept. The thickness of the fourth layer, h_4, is omitted due to its infinite depth. Associated with multiple-regression is the multiple correlation coefficient, which is the variance of the dependent variable explained collectively by all of the independent variables. A multiple-regression model, for the 4-layered soil case, is obtained using an Excel spreadsheet and is found to be best described by

$$q_u = 2.871c_1 + 1.393c_2 + 0.620c_3 + 0.426c_4 + 1.137h_1 + 0.631h_2 - 0.319h_3 - 1.061B - 4.422 \quad (12)$$

Power or exponential terms can be added as independent variables to explore curvilinear effects, and, thus two additional multiple-regression models are obtained as follows:

$$\ln q_u = 0.139c_1 + 0.058c_2 + 0.026c_3 + 0.016c_4 + 0.030h_1 + 0.020h_2 - 0.014h_3 - 0.032B + 1.790 \quad (13)$$

and

$$\ln q_u = 0.663\ln c_1 + 0.282\ln c_2 + 0.122\ln c_3 + 0.089\ln c_4 + 0.030h_1 + 0.015h_2 - 0.014h_3 - 0.029B + 1.297 \quad (14)$$

An alternative model is examined, again facilitated by the use of Excel, which involves including cross-product terms that are added as independent variables to explore interaction effects, and yield:

$$\ln q_u = 0.570\ln c_1 \cdot h_1 + 0.245\ln c_2 \cdot h_2 + 0.095\ln c_3 \cdot h_3 + 0.083\ln c_4 - 0.859h_1 - 0.366h_2 - 0.151h_3 - 0.079\ln B + 2.952 \quad (15)$$

The scatterplots of predicted versus actual values using Eqs. (12)–(15) are presented in Fig. 7. The performance of these models is assessed by using three standard performance measures, namely the correlation coefficient, r, the root mean square error, RMSE, and mean absolute error, MAE. A summary of the performance results is presented in Table 1. It is shown that, whilst all models perform well, Eq. (15) performs the best with the highest correlation coeffi-

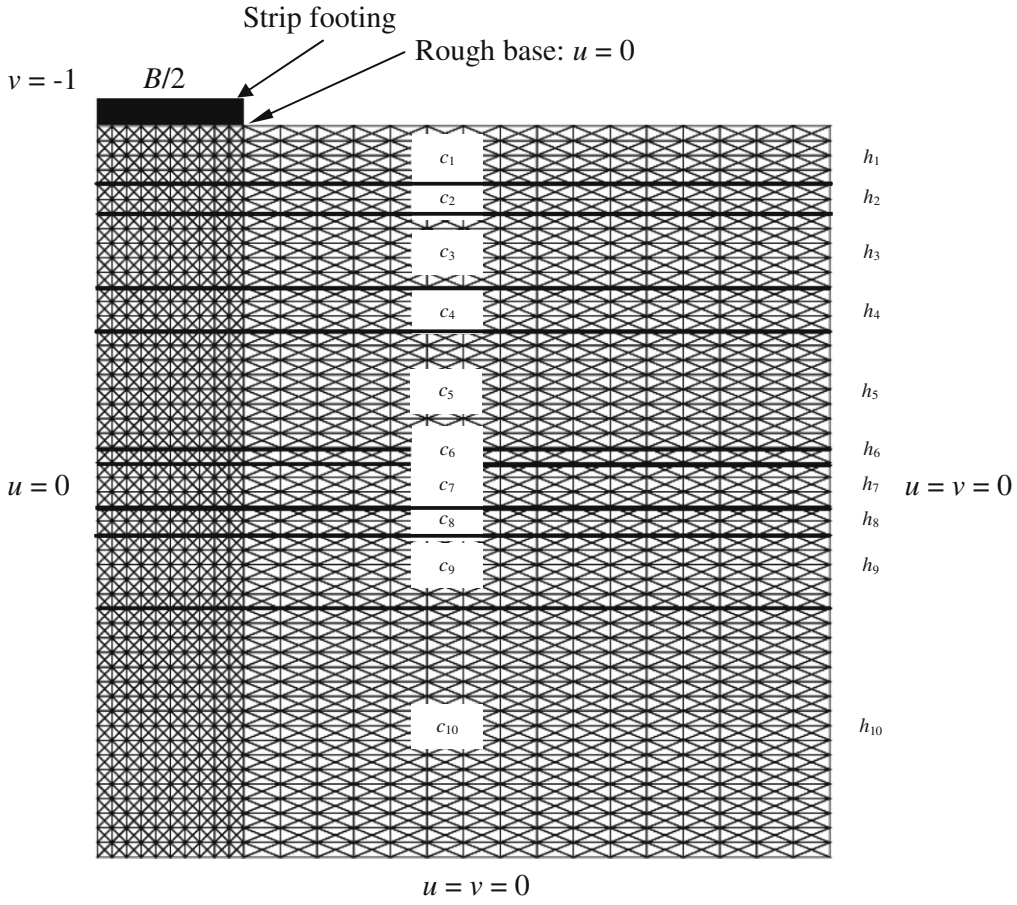

Fig. 4. Typical mesh for upper bound implementation.

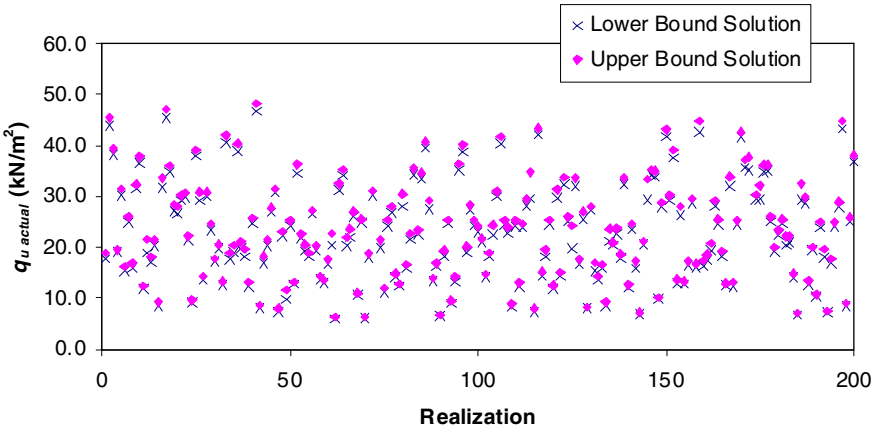

Fig. 5. Bearing capacity for the first 200 realizations (4-layer case).

cient (i.e. 0.889) and the lowest RMSE and MAE, which of 4.62 and 3.42 kN/m^2, respectively.

As will be demonstrated later, the multiple regression models perform poorly when compared to the ANN models developed below. In the case of the 10-layered soil profile, a multiple regression model is not represented here, as its predictive performance is particularly poor.

6. Development of neural network models

In order to develop a more accurate model, artificial neural networks (ANNs) are adopted. In this study, ANN models are developed using the NEUFRAME computer software [24]. For the 4-layered soil profile, eight variables are presented to the MLP models as model inputs. These include the cohesion of the four soil layers, c_1, c_2, c_3 and c_4, the stratum thickness of the three uppermost layers, h_1, h_2, and h_3, and the footing width, B (as shown in Fig. 1). For the 10-layered soil profile case, there are 20 model inputs, which include the 10 soil cohesions, $c_{1,2,\ldots,10}$, 9 stratum thicknesses $h_{1,2,\ldots,9}$, and the footing width, B (as shown in Fig. 1). For the 4- and 10-layered soil profile, the sole model output is the ultimate bearing capacity, q_u. The parameters h_4 for the 4-layer case and h_{10} for the 10-layer case are omitted from the MLP models because of their infinite depth.

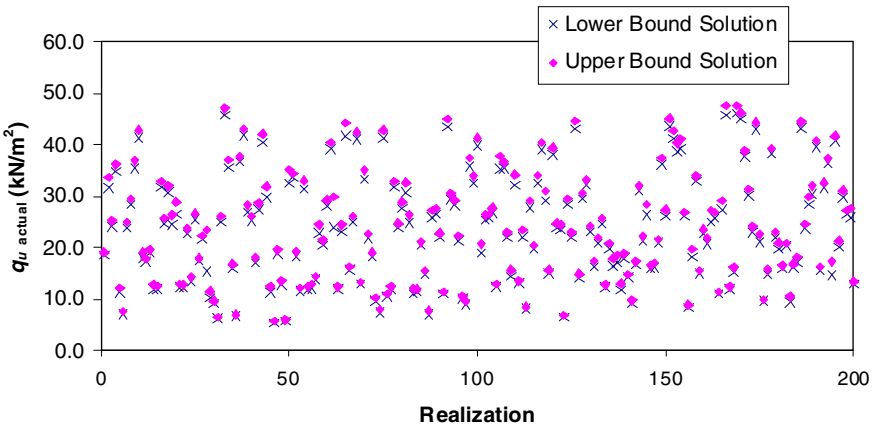

Fig. 6. Bearing capacity for the first 200 realizations (10-layer case).

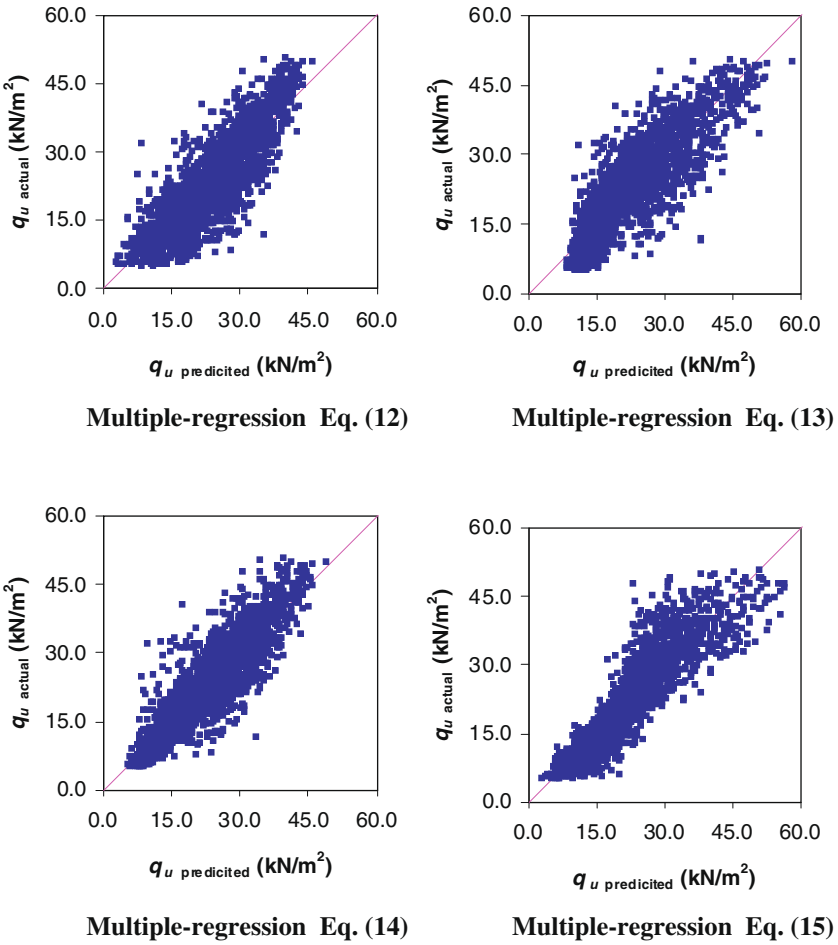

Fig. 7. Scatterplots of predicted versus actual values for 4-layered clay case using multiple-regression, Eqs. (12)–(15).

Table 1
Performance results of multiple regression models for 4-layered cohesive soils

Eqs.	r	RMSE (kN/m^2)	MAE (kN/m^2)
(12)	0.843	5.37	4.23
(13)	0.837	5.56	4.38
(14)	0.883	4.72	3.54
(15)	0.889	4.62	3.42

As cross-validation [22] is used as the stopping criterion for MLP models, the data are divided into three sets, namely: training, testing and validation. When dividing the data into their subsets, it is essential to check that the data used for training, testing and validation represent the same population, as recommended by Masters [25]. The statistics of the data used for training, testing and validation sets are presented in Table 2. In total, 80% (or 1,600 cases) of the data are used for training and 20% or (400 cases) are used for validation. The training data are further divided into

70% (i.e. 1120 cases) for the training set and 30% (480 cases) for the testing set.

Once the available data have been divided into their subsets, the input and output variables are pre-processed by scaling them between 0.0 and 1.0 to eliminate their dimension and to ensure that all variables receive equal attention during training [25]. A simple linear mapping of the variables' practical extreme to the neural networks' practical extreme is adopted for scaling, as it is the most common method for this purpose [25]. As part of this method, for each variable, x, with minimum and maximum values of x_{min} and x_{max}, respectively, the scaled value, x_n, is calculated as follows:

$$x_n = \frac{x - x_{min}}{x_{max} - x_{min}} \quad (16)$$

A network with one hidden layer can approximate any continuous function, provided that sufficient connection weights are used [26,27]. Consequently, one hidden layer is used in this paper.

A number of trials are carried out using NEUFRAME's default parameters, with one hidden layer and between 1 and 17 hidden layer nodes for the 4-layered case. Note that, as suggested by Caudill [28], $(2I + 1)$ is the upper limit for a network with I inputs to map any continuous function. Consequently, for the 10-layered case, which has 20 input variables, a maximum number of 41 is used as the upper limit of the number of hidden layer nodes. For each MLP model with a different number of hidden nodes, the strategy used for assessing the optimum MLP model is that a model is deemed to be optimal if it performs well with respect to the testing set, the model has a minimal number of hidden layer nodes, and the model has consistent performance with the validation set as with that obtained on the training and testing sets.

The results of the networks' performance, in relation to the number of hidden layer nodes, are shown in Figs. 8 and 9, and also summarised in Tables 3 and 4, using the same performance measures as used in the previous section.

It can be seen from Fig. 8, for the 4-layer case, that the number of hidden layer nodes has a significant impact on the predictive ability of the ANN model. For networks with three or less hidden layer nodes, the ability of the model to adequately map the underlying relationship is less than satisfactory. For networks with a larger number of hidden layer nodes, the predictive error is reduced as the number of nodes increases. Fig. 8 also shows that the network with 16 hidden layer nodes has the lowest prediction error, for the 4-layer case. However, in the interest of developing a parsimonious model, a network with five hidden layer nodes is considered optimal for a 4-layered soil profile, and consequently, a network with seven hidden layers nodes is selected for a 10-layered soil profile. The structures of the MLP models are shown in Figs. 10 and 11.

Table 2
ANN input and output statistics for 4-layered case

Model variable and data sets	Mean	Standard deviation	Minimum	Maximum	Range
Soil cohesion at layer 1 (c_1) (kPa)					
Training set	5.53	2.55	1.01	10.00	8.99
Testing set	5.44	2.48	1.02	9.99	8.97
Validation set	5.49	2.61	1.03	9.98	8.95
Soil cohesion at layer 2 (c_2) (kPa)					
Training set	5.53	2.61	1.00	9.99	8.99
Testing set	5.66	2.55	1.03	9.96	8.93
Validation set	5.54	2.63	1.00	9.98	8.98
Soil cohesion at layer 3 (c_3) (kPa)					
Training set	5.52	2.64	1.00	10.00	9.00
Testing set	5.55	2.58	1.00	9.97	8.97
Validation set	5.71	2.62	1.00	9.99	8.99
Soil cohesion at layer 4 (c_4) (kPa)					
Training set	5.54	2.64	1.01	9.99	8.98
Testing set	5.49	2.74	1.01	9.99	8.98
Validation set	5.62	2.61	1.01	9.99	8.98
Soil thickness of layer 1 (h_1) (m)					
Training set	1.04	0.58	0.10	2.00	1.90
Testing set	1.03	0.58	0.10	2.00	1.90
Validation set	1.03	0.60	0.10	2.00	1.90
Soil thickness of layer 2 (h_2) (m)					
Training set	1.05	0.59	0.10	2.00	1.90
Testing set	1.04	0.58	0.10	2.00	1.90
Validation set	1.03	0.57	0.10	2.00	1.90
Soil thickness of layer 3 (h_3) (m)					
Training set	1.03	0.58	0.10	2.00	1.90
Testing set	1.02	0.57	0.10	2.00	1.90
Validation set	1.02	0.56	0.10	2.00	1.90
Footing width (B) (m)					
Training set	2.50	0.93	1.00	4.00	3.00
Testing set	2.53	0.94	1.00	4.00	3.00
Validation set	2.60	0.91	1.00	4.00	3.00
Average bearing capacity of strip footing (q_u) (kN/m^2)					
Training set	23.75	9.83	5.27	50.35	45.08
Testing set	23.85	10.55	5.52	50.08	44.56
Validation set	23.71	9.82	5.57	50.07	44.50

7. Bearing capacity equation

In order to facilitate the use of the developed MLP models, they are translated into a set of relatively simple equations, suitable for

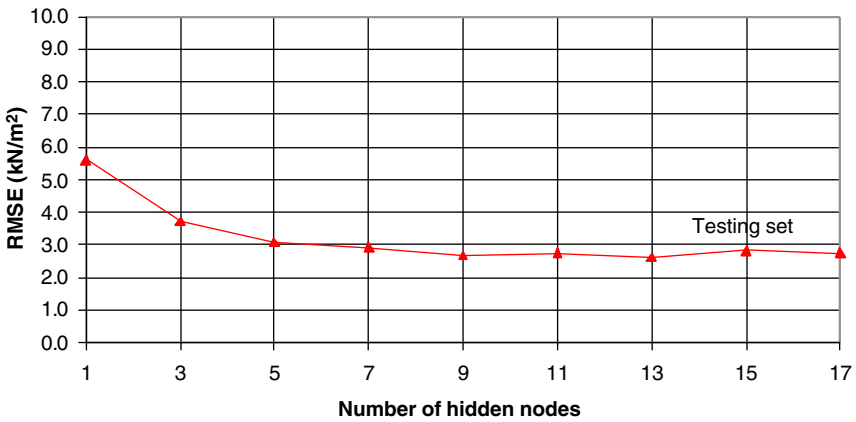

Fig. 8. Root mean square error versus number of hidden layer nodes for the 4-layer-case.

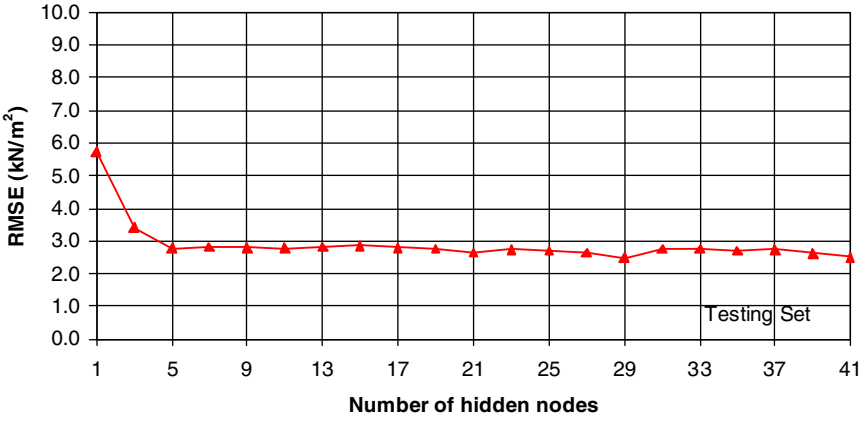

Fig. 9. Root mean square error versus number of hidden layer nodes for the 10-layer-case.

Table 3
Performance results of ANN models for 4-layered soils

Model number	Number hidden layer nodes	Data sets								
		Training set			Testing set			Validation set		
		Performance measures								
		r	RMSE (kN/m^2)	MAE (kN/m^2)	r	RMSE (kN/m^2)	MAE (kN/m^2)	r	RMSE (kN/m^2)	MAE (kN/m^2)
NF_4_1	1	0.846	5.324	4.219	0.853	5.605	31.41	0.832	5.494	30.18
NF_4_3	3	0.937	3.535	2.568	0.945	3.718	13.82	0.921	3.957	15.65
NF_4_5	5	0.955	2.951	2.191	0.959	3.096	9.587	0.946	3.222	10.38
NF_4_7	7	0.965	2.683	1.977	0.966	2.938	8.634	0.953	3.104	9.634
NF_4_9	9	0.971	2.489	1.853	0.971	2.687	7.221	0.961	2.932	8.594
NF_4_11	11	0.969	2.577	1.930	0.972	2.755	7.590	0.961	2.869	8.230
NF_4_13	13	0.969	2.460	1.806	0.971	2.624	6.883	0.961	2.767	7.657
NF_4_15	15	0.969	2.608	1.931	0.969	2.824	7.973	0.957	3.008	9.047
NF_4_17	17	0.970	2.548	1.864	0.970	2.747	7.547	0.958	2.960	8.762

Table 4
Performance results of ANN models for 10-layered soils

Model number	Number hidden layer nodes	Data sets								
		Training set			Testing set			Validation set		
		Performance measures								
		r	RMSE (kN/m^2)	MAE (kN/m^2)	r	RMSE (kN/m^2)	MAE (kN/m^2)	r	RMSE (kN/m^2)	MAE (kN/m^2)
NF_10_1	1	0.860	5.521	4.290	0.857	5.724	32.76	0.863	5.928	35.14
NF_10_3	3	0.945	3.431	2.567	0.944	3.421	11.70	0.941	3.803	14.46
NF_10_5	5	0.963	2.769	2.100	0.961	2.780	7.727	0.961	3.053	9.319
NF_10_7	7	0.964	2.689	2.048	0.959	2.829	8.003	0.962	2.955	8.735
NF_10_9	9	0.965	2.733	2.070	0.961	2.803	7.856	0.962	3.037	9.224
NF_10_11	11	0.968	2.561	1.980	0.961	2.781	7.733	0.963	2.966	8.795
NF_10_13	13	0.968	2.617	2.000	0.961	2.829	8.004	0.963	2.962	8.776
NF_10_15	15	0.969	2.562	1.983	0.959	2.855	8.149	0.963	2.963	8.780
NF_10_17	17	0.968	2.590	1.978	0.960	2.793	7.802	0.963	2.980	8.883
NF_10_19	19	0.968	2.552	1.942	0.961	2.760	7.617	0.965	2.857	8.165
NF_10_21	21	0.975	2.317	1.786	0.965	2.627	6.904	0.967	2.809	7.888
NF_10_23	23	0.970	2.502	1.907	0.962	2.729	7.445	0.964	2.911	8.476
NF_10_25	25	0.970	2.493	1.901	0.963	2.704	7.311	0.964	2.899	8.403
NF_10_27	27	0.974	2.453	1.882	0.965	2.637	6.954	0.966	2.909	8.463
NF_10_29	29	0.975	2.320	1.797	0.969	2.485	6.176	0.968	2.790	7.782
NF_10_31	31	0.971	2.597	2.012	0.962	2.755	7.592	0.965	2.967	8.805
NF_10_33	33	0.968	2.593	1.996	0.962	2.753	7.577	0.961	2.996	8.976
NF_10_35	35	0.971	2.479	1.902	0.962	2.709	7.340	0.963	2.908	8.458
NF_10_37	37	0.970	2.488	1.910	0.962	2.735	7.480	0.962	2.926	8.561
NF_10_39	39	0.975	2.310	1.773	0.965	2.613	6.826	0.964	2.867	8.220
NF_10_41	41	0.980	2.112	1.637	0.968	2.505	6.277	0.970	2.642	6.981

hand calculation. The form of the equations, and relative weights, are provided as output by the NEUFRAME software. Note that both the inputs and output need to be rescaled, in order to use the actual values for input and to obtain the bearing capacity.

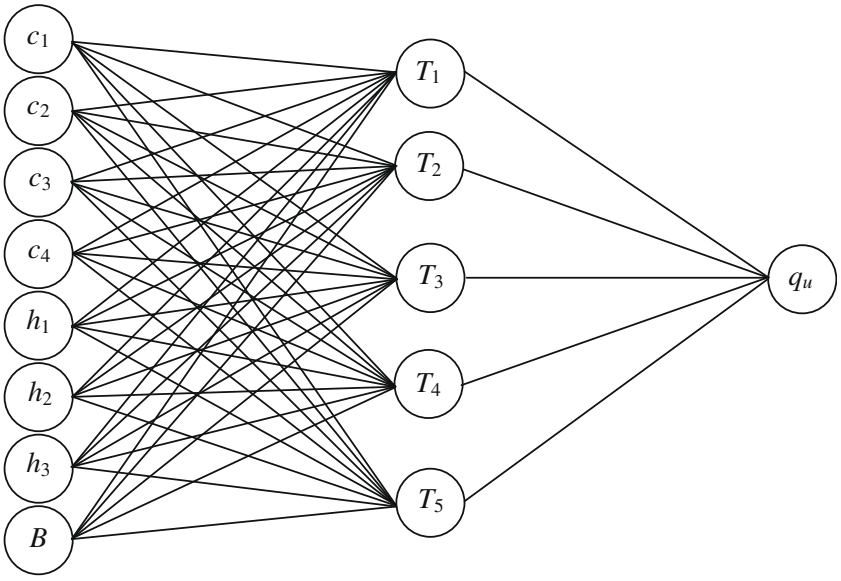

Units: c_i in kPa; h_i and B in m and q_u in kN/m^2.

Fig. 10. Structure of the optimum MLP model for 4-layered cohesive soil.

For the 4-layered cohesive soil, with reference to Fig. 10 , the optimal MLP model can be expressed as

$$q_u = \left[\frac{45.53}{\{1+\exp(-1.994T_1 - 4.232T_2 + 3.295T_3 + 3.992T_4 + 4.758T_5 - 1.396)\}} + 5.27\right] \times a \tag{17}$$

where parameter a is an introduced scalar quantity defined by $c_{min} < ac_i < c_{max}$, such that $1.0 < c_i < 10.0$ kPa. In reality, the soil cohesion has a wide range and therefore, in order to improve the applicability of the resulted MLP models, the parameter a, has been introduced. This is illustrated later by means of a numerical example. The parameter $T_{i=1,\ldots,5}$ represents the hidden layer nodes, as shown in Fig. 10 and is defined as

$$T_{i=1,\ldots,5} = [1+\exp(a^{-1}(w_1c_1 + w_2c_2 + w_3c_3 + w_4c_4) + w_5h_1 + w_6h_2 + w_7h_3 + w_8B + C)]^{-1} \tag{18}$$

and the coefficients $w_{1,\ldots,8}$ and C, for $T_{1,\ldots,5}$, are given in Table 5 and, together with the parameter a, they are all dimensionless.

For the 10-layered cohesive soil, with reference to Fig. 11, the optimal MLP model is expressed as follows:

$$q_u = \left\{\frac{46.11}{1+\exp(-5.183T_1 + 3.834T_2 - 1.845T_3 + 4.158T_4 - 0.311T_5 - 1.704T_6 + 3.787T_7 + 1.402)} + 5.15\right\} \times a \tag{19}$$

where $T_{i=1,\ldots,7}$ again represents the hidden layer nodes, as shown in Fig. 11 and is expressed as

$$T_{i=1,\ldots,7} = \{1+\exp[a^{-1}(w_1c_1 + w_2c_2 + w_3c_3 + w_4c_4 + w_5c_5 + w_6c_6 + w_7c_7 + w_8c_8 + w_9c_9 + w_{10}c_{10}) + w_{11}h_1 + w_{12}h_2 + w_{13}h_3 + w_{14}h_4 + w_{15}h_5 + w_{16}h_6 + w_{17}h_7 + w_{18}h_8 + w_{19}h_9 + w_{20}B + C]\}^{-1} \tag{20}$$

The coefficients $w_{1,\ldots,20}$ and C for $T_{i=1,\ldots,7}$ are given in Table 4. The parameter q_u is the predicted bearing capacity (kN/m^2); B is the width of shallow strip footing (m); c_i is the soil cohesion in each layer (kPa); and h_i is the thickness of the stratum (m). As in the previous model, each of the parameters $T_{i=1,\ldots,7}$, a, w_i and C are dimensionless.

It is worthwhile to note that the prediction ability of MLP models is better when used for ranges of values of B and h_i given in Table 6. This is because ANNs work best when used in interpolation rather than extrapolation, as mentioned earlier.

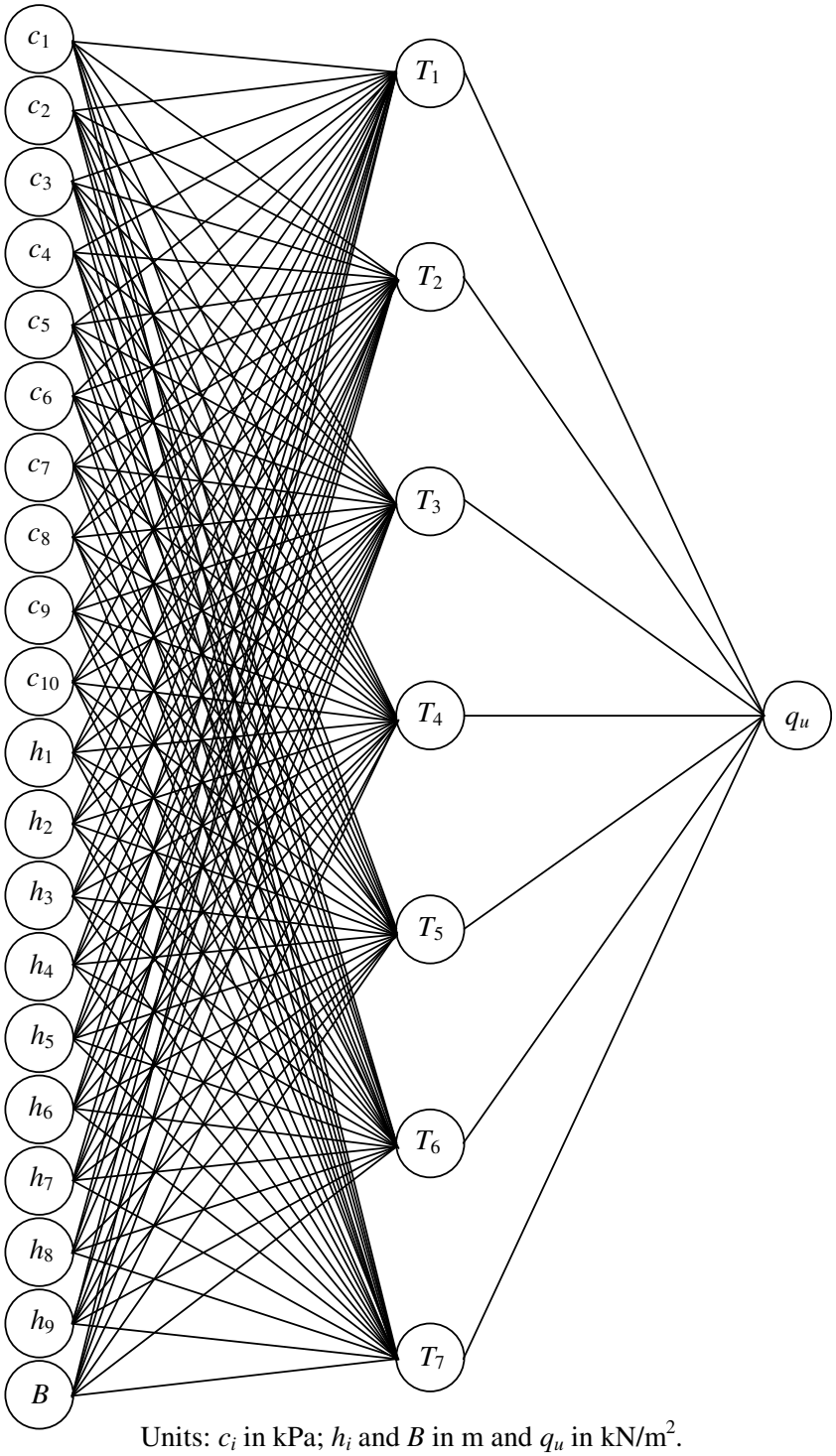

Units: c_i in kPa; h_i and B in m and q_u in kN/m^2.

Fig. 11. Structure of the optimum MLP model for 10-layered cohesive soil.

8. Sensitivity and robustness of the MLP-based bearing capacity equations

As proposed by Shahin et al. [29], in order to test the robustness of the predictive ability of the MLP model and, consequently, the MLP-based bearing capacity design formula, a sensitivity analysis is carried out over a range of data valid for the model (i.e. within the minimum and maximum ranges given in Table 2). The sensitivity analysis investigates the response of the predicted bearing capacity from the ANN model to a set of hypothetical input data that are generated over the ranges of the minimum and maximum data used for the MLP model training. All input variables, except one, are fixed to a certain chosen value, and a set of synthetic data for the single varied input is generated by increasing the value of this in increments. These inputs are presented to Eqs. (17)–(20) and the bearing capacity is calculated. This process is repeated using another input variable until the model response is tested for all input variables. The robustness of the design equation is

Table 5
Value of $w_{i=1,\ldots,8}$ and C versus $T_{i=1,\ldots,5}$ for 4-layer-case

	T_1	T_2	T_3	T_4	T_5
w_1	0.090	0.218	−0.094	0.319	−0.416
w_2	−0.015	0.274	0.086	−0.207	0.284
w_3	0.060	−0.163	0.033	−0.210	0.006
w_4	0.096	−0.109	0.042	−0.106	−0.002
w_5	0.309	−0.493	−1.622	−0.396	1.047
w_6	−0.175	−0.804	−0.044	−0.494	−0.405
w_7	−0.635	0.143	−0.075	−0.203	0.015
w_8	−0.169	0.424	0.736	0.283	−0.297
C	−0.21	−1.16	−0.59	1.22	0.12

Table 6
Value of $w_{i=1,\ldots,20}$ and C versus $T_{i=1,\ldots,7}$ for 10-layer-case

	T_1	T_2	T_3	T_4	T_5	T_6	T_7
w_1	0.424	0.141	0.036	−0.080	0.026	0.048	−0.032
w_2	−0.151	−0.117	−0.001	0.063	0.029	−0.032	−0.343
w_3	−0.044	−0.210	0.090	0.038	−0.036	0.077	0.177
w_4	−0.021	−0.048	0.034	0.005	−0.016	0.026	0.027
w_5	−0.019	−0.020	0.039	0.032	0.007	0.026	0.003
w_6	0.001	−0.021	−0.024	0.015	−0.018	0.006	−0.014
w_7	0.013	−0.030	−0.004	0.030	−0.012	−0.029	−0.015
w_8	0.005	0.001	−0.024	−0.017	0.005	−0.023	−0.015
w_9	0.007	−0.021	−0.081	−0.001	−0.009	0.009	−0.023
w_{10}	0.008	−0.010	−0.032	0.010	−0.046	0.052	0.007
w_{11}	−1.022	−0.465	−0.105	−1.287	0.099	−0.409	−0.045
w_{12}	−0.036	−0.262	0.427	−0.152	0.254	0.200	0.842
w_{13}	−0.022	0.192	0.109	0.088	0.237	0.030	−0.232
w_{14}	0.044	−0.066	0.190	0.097	0.152	−0.128	0.086
w_{15}	−0.081	0.085	0.055	0.035	0.181	0.245	−0.035
w_{16}	0.082	−0.058	−0.261	−0.037	−0.191	0.056	0.022
w_{17}	−0.076	0.029	0.098	−0.148	−0.286	0.000	0.048
w_{18}	−0.082	0.101	0.229	−0.018	−0.263	0.219	0.031
w_{19}	−0.016	−0.071	0.084	−0.031	−0.006	−0.120	0.067
w_{20}	0.418	0.094	−0.179	0.691	0.029	−0.089	−0.227
C	−0.71	−0.34	0.10	0.55	−0.22	−0.18	0.30

determined by examining how well the predicted bearing capacities agree with the underlying physical behaviour of the bearing capacity of a shallow strip footing.

The results of the sensitivity analysis are shown in Figs. 12–14 for the 4-layer case, and Figs. 15–17 for the 10-layer case. The results indicate that the behaviour of the MLP model is in good agreement with what one would expect based on the physical behaviour of the bearing capacity problem. For example, in Figs. 12 and 15 , where the cohesion in 3 of the layers remain constant at 10 kPa and the cohesion in the remaining layer is varied from 1 to 10 kPa, it can be seen that there is an increase in the bearing capacity as the soil cohesion increases in one layer while the soil strength remains constant in the other layers. This is expected, by theory, as an increase in soil shear strength provides greater bearing capacity of the footing. Figs. 12 and 15 also indicated that a change of soil strength and stratum thickness in the uppermost layer has the most significant impact on bearing capacity, compared to the variation in the other layers, as one would expect. In Figs. 14 and 17, it can be seen that the bearing capacity is higher for larger widths of footing. This is because, as the surface area of the footing increases, the magnitude of the load that can be applied to the footing also increases. In addition, in Figs. 12 and 15, it can be observed that the estimate of q_u plateaus at ≈45 kN/m^2, when all soil layers have the same c_u = 10 kPa. Theoretically, however, q_u should reach approximately 51.4 kN/m^2 ($q_u = 5.14c_u$). These results demonstrate the numerical inaccuracy associated with the model when all soil layers have the same value of c_u. Whilst this error is undesirable, the ANN model is developed primarily to predict the bearing capacity of soil layers having different values of c_u.

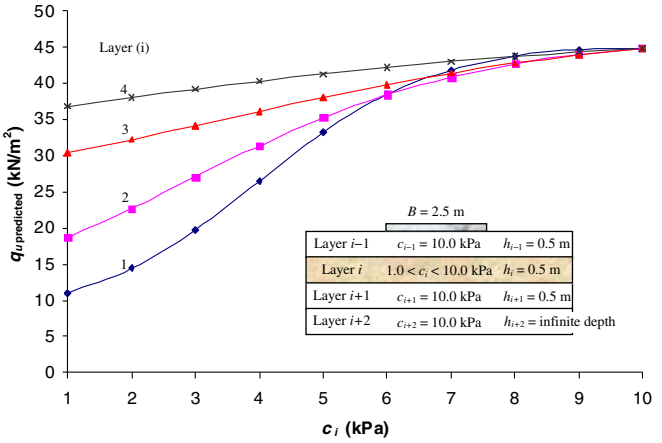

Fig. 12. Variation of q_u versus varying soil cohesion in one of the 4 layers. [*Note*: Curve i represents the predicted ultimate bearing capacity when the soil cohesion for layer i varies from 1.0 to 10.00 kPa, with the cohesion of the other layers remaining constant at 10 kPa.]

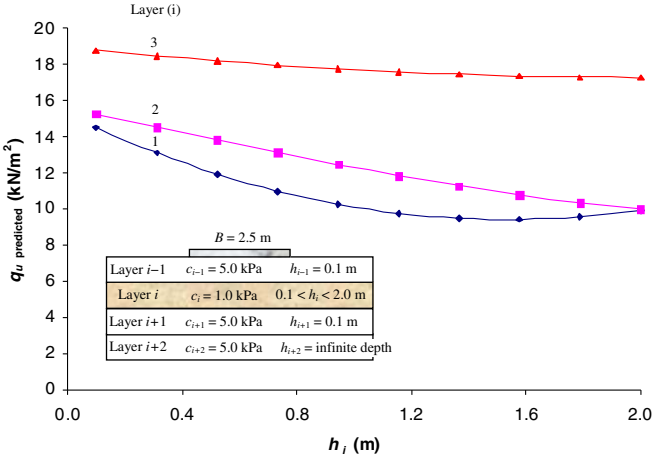

Fig. 13. Variation of q_u versus varying layer thickness, h_i.

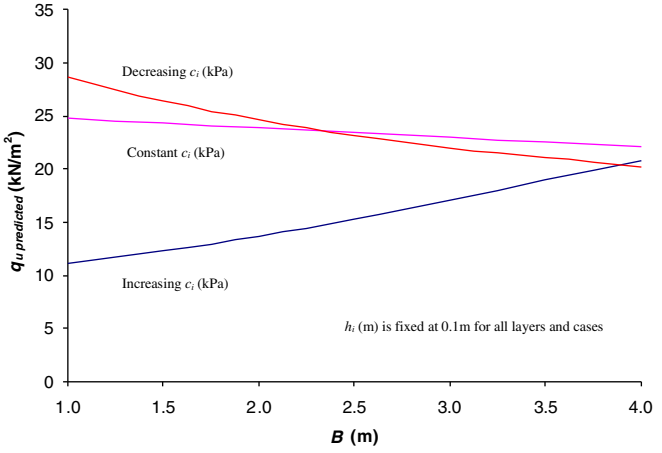

Fig. 14. Variation of q_u versus B and c_i (4-layer case).

In summary, the results indicate that the bearing capacity of a footing on multi-layered soils increases as the soil cohesion increases; and as the width of the footing increases; and are strongly influenced by the soil layers located immediately beneath the foot-

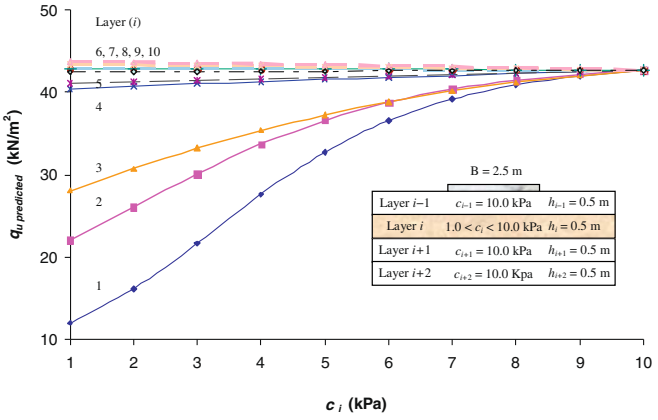

Fig. 15. Variation of q_u versus varying soil cohesion in one of the 10 layers.

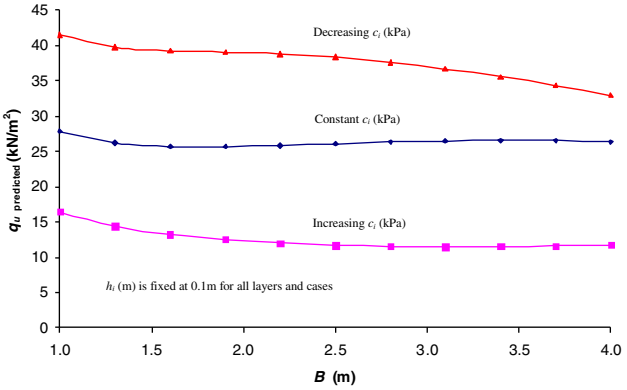

Fig. 17. Variation of q_u versus B and c_i (10-layer case).

ing. The above results confirm that the MLP-based design formula is robust and can be used confidently for predictive purposes within the range of the input variables given in Table 2. It should be noted however that, while the models were developed within the ranges given in Table 2, it is possible to extend the models to situation beyond these ranges by the use of the scalar, a, introduced in Eqs. (18) and (20).

9. Comparison of MLP models with current methods

In order to examine the accuracy of the MLP model, it is compared with the other methods, namely the multiple-regression and Bowles [12] methods. The performances of the MLP models and the other methods, in relation to the data set of 2000 multi-layered bearing capacity cases, obtained from the upper and lower bound implementations, are summarised in Table 7 and Figs. 18–21. It can be seen, from Figs. 20 and 21, that the MLP models outperform the other methods, as they exhibit less scatter about the line of equality between the actual and predicted bearing capacities. The *actual* bearing capacities, denoted as $q_{u\ actual}$, are the results obtained from finite element limit analysis, whereas the predicted bearing capacities, denoted as $q_{u\ predicted/calculated}$, are the results obtained from employing either the MLP model, multiple-regression or Bowles [12] methods. The weighted average, or Bowles [12] method, appears to over-estimate the bearing capacity of a footing resting on both 4-layered and 10-layered soil profiles, as shown in Figs.18 and19, when compared to the results obtained from finite element limit analysis. This is also shown by the results in Table 7, which indicate that the MLP models have relatively higher coefficients of correlation between the actual and predicted bearing capacities of 0.967 and 0.974 for the 4- and 10-layered soil, respectively. In contrast, when other methods are used, the correlation coefficients ranged from 0.869 to 0.889. When the MLP model is used in a 4-layered soil, the RMSE and MAE are determined to be equal 2.43 and 1.86 kN/m^2, respectively, and, for 10-layered soil case, the RMSE and MAE are found to be equal to 2.30 and 1.73 kN/m^2, respectively. In contrast, when the other methods are used, the RMSE and MAE ranged from 4.62 to 7.28 kN/m^2 and from 3.42 to 4.84 kN/m^2, respectively.

10. Illustrative numerical example

An illustrative numerical example is provided to explain better the implementation of the bearing capacity formula. A strip footing of width 1.8 m rests on a 10-layered soil with $c_{i=1,\ldots,10}$ of 83.96, 81.68, 82.86, 18.49, 52.41, 98.86, 25.70, 28.02, 41.17, 83.65 kPa, respectively; and $h_{i=1,\ldots,9}$ are 0.7, 0.3, 0.5, 0.4, 1.0, 0.1, 0.2, 0.5, 0.9 m, respectively. The ultimate bearing capacity of strip footing is required.

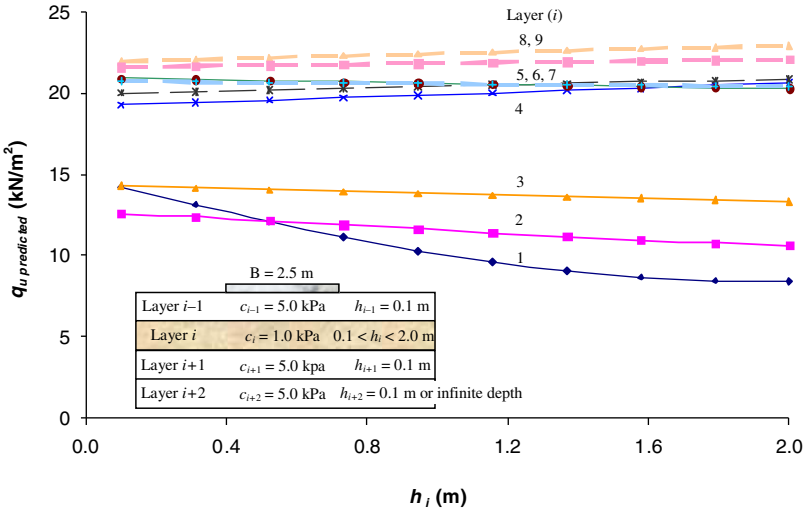

Fig. 16. Variation of q_u versus varying layer thickness, h_i (10-layer-case).

Table 7
Comparison of ANN and other methods for bearing capacity prediction

Performance measure	Method				
	4-Layer case			10-Layer case	
	MLP	Multiple-regression	Bowles [12]	MLP	Bowles [12]
Correlation coefficient, r	0.959	0.889	0.869	0.959	0.879
RMSE (kN/m^2)	3.10	4.62	7.25	2.83	7.28
MAE (kN/m^2)	9.59	3.42	4.84	8.00	4.81

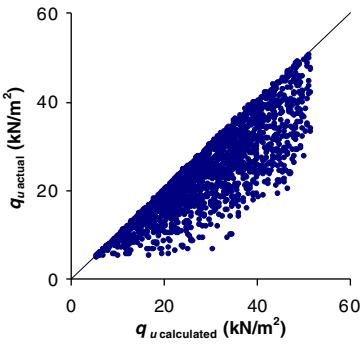

Fig. 18. Comparison of the predicted bearing capacity calculated using the averaging method of Bowles [12] versus the actual values from the lower and upper bound implementation for the 4-layered clay case.

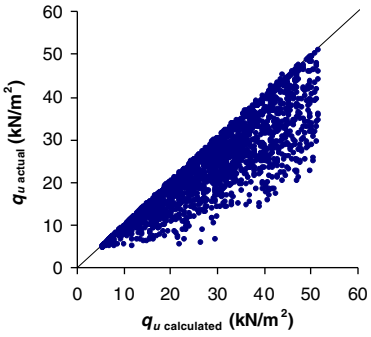

Fig. 19. Comparison of the predicted bearing capacity calculated using the averaging method of Bowles [12] versus the actual values from the lower and upper bound implementation for the 10-layered clay case.

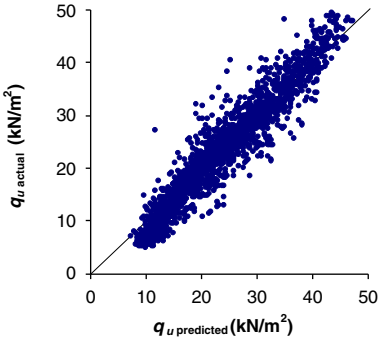

Fig. 20. Actual versus predicted bearing capacity for the MLP model for the 4-layered case.

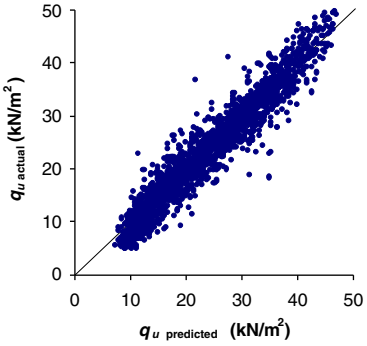

Fig. 21. Actual versus predicted bearing capacity for the MLP model for the 10-layered case.

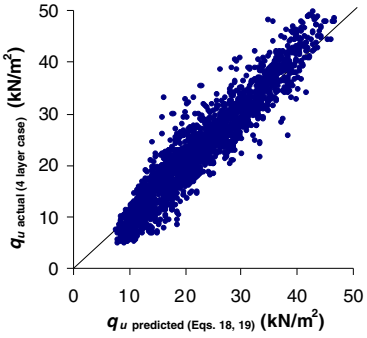

Fig. 22. Actual bearing capacity for 4-layered case versus predicted bearing capacity using the MLP models Eqs. (19) and (20) for the 10-layered case.

10.1. Solution

Given the information provided, $a = 10$ is suggested such that $c_{min} = 10$ kN/m^2 and $c_{max} = 100$ kN/m^2 and the ratio c_{min}/c_{max} is equal to 0.1. Eqs. (19) and (20) are applied as follows:

$$\begin{aligned} T_1 = \{1 + \exp[10^{-1}(&-0.424 \times 83.96 + 0.151 \times 81.68 + 0.044 \\ &\times 82.62 + 0.021 \times 18.49 + 0.019 \times 52.41 - 0.001 \times 98.86 \\ &- 0.013 \times 25.70 - 0.005 \times 28.02 - 0.007 \times 41.17 - 0.008 \\ &\times 83.65) + 1.022 \times 0.7 + 0.036 \times 0.3 + 0.022 \times 0.5 - 0.044 \\ &\times 0.4 + 0.081 \times 1.0 - 0.082 \times 0.1 + 0.076 \times 0.2 + 0.082 \\ &\times 0.5 + 0.016 \times 0.9 - 0.418 \times 1.80 + 0.71]\}^{-1} \\ = 0.930 \end{aligned}$$

Similarly, $T_2 = 0.229$, $T_3 = 0.616$, $T_4 = 0.883$, $T_5 = 0.421$, $T_6 = 0.662$ and $T_7 = 0.079$. Substituting $T_{i=1,\ldots,7}$ into equation, the bearing capacity can be obtained as follows:

$$q_u = \{46.11 \times [1 + \exp(-5.183 \times 0.930 + 3.834 \times 0.229 - 1.845 \times 0.616 + 4.158 \times 0.883 - 0.311 \times 0.421 - 1.704 \times 0.662 + 3.787 \times 0.079 + 1.402)]^{-1} + 5.15\} \times 10 = 385.7 \text{ kN/m}^2$$

Hence, in this example, the result is in reasonable good agreement with the numerical finite limit analysis, yields a value 18% lower (326.1 kN/m^2).

11. Compatibility of Eqs. (18) and (19)

In reality, the soil profiles may consists of 4 to 10 layers. When developing ANN models, ideally, only one general model is required for all cases. Consequently, this section examines the compatibility of ANN models for 10-layer-case (Eqs. (19) and (20)) to predict the bearing capacity for all cases. By using this model, predictions on bearing capacity of 4-layer-case are made and then compared to the actual values. The values of $c_{i=1,\ldots,4}$ and $h_{i=1,\ldots,3}$ in (Eqs. (19) and (20)) are assigned corresponding to the actual values of 4-layer soil profiles, while the values of $c_{i=5,\ldots,10}$ are set to be same as c_4, and $h_{i=4,\ldots,9}$ to be 0.10 m, which is the minimum of the range values.

For example, a strip footing of width 2.60 m rests on a 4-layered soil with $c_{i=1,\ldots,4}$ of 3.37, 7.69, 1.81 and 6.04 kPa, respectively; and $h_{i=1,\ldots,3}$ are 1.20, 1.70 and 1.20, respectively. Given the information provided, and selecting $a = 1$, Eq. (20) is applied as follows:

$$T_1 = \{1 + \exp[10^{-1}(-0.424 \times 3.37 + 0.151 \times 7.69 + 0.044 \times 1.81 + 0.021 \times 6.04 + 0.019 \times 6.04 - 0.001 \times 6.04 - 0.013 \times 6.04 - 0.005 \times 6.04 - 0.007 \times 6.04 - 0.008 \times 6.04) + 1.022 \times 1.20 + 0.036 \times 1.70 + 0.022 \times 1.20 - 0.044 \times 0.10 + 0.081 \times 0.10 - 0.082 \times 0.10 + 0.076 \times 0.10 + 0.082 \times 0.10 + 0.016 \times 0.10 - 0.418 \times 2.60 + 0.71]\}^{-1} = 0.511$$

and, $T_2 = 0.209$, $T_3 = 0.563$, $T_4 = 0.718$, $T_5 = 0.581$, $T_6 = 0.439$ and $T_7 = 0.099$. Substituting $T_{i=1,\ldots,7}$ into Eq. (19), and yield:

$$q_u = \{46.11 \times [1 + \exp(-5.183 \times 0.511 + 3.834 \times 0.209 - 1.845 \times 0.563 + 4.158 \times 0.718 - 0.311 \times 0.581 - 1.704 \times 0.439 + 3.787 \times 0.099 + 1.402)]^{-1} + 5.15\} \times 1 = 17.99 \text{ kN/m}^2$$

Hence, the result is in good agreement with the numerical finite limit analysis, yields a value 2% higher (18.34 kN/m^2). The results of predicted versus actual bearing capacity over 2,000 realization is shown in Fig. 22. The correlation coefficient is found to be 0.947 while the RMSE and MAE are determined to be equal 3.35 and 2.59 kN/m^2, respectively, and, for 10-layered soil case, the RMSE and MAE are found to be equal to 2.83 and 8.00 kN/m^2, respectively. It shows MLP model for 10-layer can be used confidently for 4 to 10-layer soil profile.

12. Summary and conclusions

The feasibility of utilising the artificial neural network (ANN) technique for predicting the bearing capacity of shallow strip footing on multi-layered soils has been assessed using multi-layer perceptions (MLPs) trained with the back-propagation algorithm.

In order to test the robustness of the developed MLP, a sensitivity analysis on each influencing factor was carried out. A new tractable design equation based on the MLP model has been derived to facilitate the use of the model. Predictions of ANN models and other methods have been compared and the results have been discussed.

The results indicate that the MLP models are able to predict well the bearing capacity of a strip footing and significantly outperform other methods. The sensitivity analysis carried out to test the robustness of the developed MLP model and consequently the MLP-based design equation indicate that the model is robust and can be used for predictive purposes with confidence.

However, both upper and lower bound computations were carried out in 2-dimensions and it was assumed that the footing has infinite length in the out of plane direction. It would be desirable to vary the length of a rectangular footing in the future so that the upgraded model can accurately predict the bearing capacity of 3D strip footings.

References

[1] Terzaghi K. Theoretical soil mechanics. New York: John Wiley & Sons; 1943.
[2] Prandtl L. Über die eindringungs-festigkeigt (Härte) plastischer bautoffe und die festigkeit von schneiden. Z Angew Math Mech 1921;1(1):15–20.
[3] Davis EH, Booker JR. The effect of increasing strength with depth on the bearing capacity of clays. Géotechnique 1973;23(4):551–63.
[4] Button SJ. The bearing capacity of footings on a two-layer cohesive subsoil. In: Proceedings of the international conference soil mechanics foundation engineering, Zurich 1953;1: p. 332–5.
[5] Chen WF. Limit analysis and soil plasticity. Amsterdam: Elsevier; 1975.
[6] Reddy AS, Srinivasan RJ. Bearing capacity of footings on layered clays. J Soil Mech Found Div ASCE 1967;93 SM2:83–99.
[7] Brown JD, Meyerhof GG. Experimental study of bearing capacity in layered clays. In: Proceedings of the 7th international conference soil mechanics foundation, Mexico 1969;2: p. 45–51.
[8] Meyerhof GG, Hanna AM. Ultimate bearing capacity of foundations on layered soils under inclined load. Can Geotech J 1978;15:565–72.
[9] Burd HJ, Frydman S. Bearing capacity of plane-strain footings on layered soils. Can Geotech J 1997;34:241–53.
[10] Florkiewicz A. Upper bound to bearing capacity of layered. Can Geotech J 1989;26:730–6.
[11] Merrifield RS, Sloan SW, Yu HS. Rigorous solutions for the bearing capacity of two layered clay soils. Géotechnique 1999;49(4):471–90.
[12] Bowles JE. Foundation analysis and design. New York: McGraw-Hill; 1988.
[13] Nagtegaal JC, Park DM, Rice JR. On numerically acquire finite element solutions in the fully plastic range. Comput Meth Appl Mech Eng 1974;4:153–77.
[14] Sloan SW, Randolph MF. Numerical prediction of collapse loads using finite element. Int J Numer Anal Meth Geomech 1982;6:47–76.
[15] Lyamin AV, Sloan SW. Upper bound limit analysis using linear finite elements and nonlinear programming. Int J Numer Anal Meth Geomech 2002;23(2): 181–216.
[16] Lyamin AV, Sloan SW. Lower bound limit analysis using linear finite elements and nonlinear programming. Int J Numer Meth Eng 2002;55(5):573–611.
[17] Lyamin AV. Three-dimensional lower bound limit analysis nonlinear programming. PhD thesis, University of Newcastle, Callaghan, NSW, Australia; 1999.
[18] Zurada JM. Introduction to artificial neural systems. St. Paul: West Publishing Company; 1992.
[19] Fausett LV. Fundamentals neural networks: architecture, algorithms, and applications. Englewood Cliffs (NJ): Prentice-Hall; 1994.
[20] Shahin MA, Jaksa MB, Maier HR. Artificial neural network application in geotechnical engineering. Aust Geomech 2001;36(1):49–62.
[21] Maier RM, Dandy GC. The effect of internal parameters and geometry on the performance of back-propagation neural networks: an empirical study. Environ Modell Software 1998;13:193–209.
[22] Stone M. Cross-validatory choice and assessment of statistical predictions. J Roy Stat Soc 1974;B 36:111–47.
[23] Smith M. Neural networks for statistical modelling. New York: Van Nostrand Reinhold; 1993.
[24] Neusciences. Neuframe version 4.0. Southhampton, Hampshire: Neusciences Co.; 2000.
[25] Masters T. Practical neural network recipes in C++. San Diego (CA): Academic Press; 1993.
[26] Cybenko G. Approximation by superpositions of a sigmoidal function. Math Contr, Signals Syst 1989;3:303–14.
[27] Hornik K, Stinchcombe M, White H. Multilayer feedforward networks are universal approximators. Neural Networks 1989;2:359–66.
[28] Caudill M. Neural network primer, part III. AI Expert 1988;3(6):53–9.
[29] Shahin MA, Maier HR, Jaksa MB. Investigation into robustness of artificial neural network models for a case study in civil engineering. In: Zerger A, Argent RM editors. MODSIM 2005 international congress on modelling and simulation. Modelling and Simulation Society of Australia and New Zealand, Dec. 2005. p. 79–83.